Sources of Error in Coplanar-Waveguide TRL Calibrations

Raian F. Kaiser and Dylan F. Williams
National Institute of Standards and Technology, 325 Broadway, Boulder CO 80303
Ph: [+1] (303) 497-5491 Fax: [+1] (303) 497-3122 E-mail: rkaiser@boulder.nist.gov

***Abstract*- This paper explores the impact of five sources of systematic error in coplanar-waveguide thru-reflect-line calibrations. We develop expressions that predict systematic measurement error and test them experimentally by deliberately introducing error into real measurement data.**

INTRODUCTION

We explore five sources of systematic error in coplanar-waveguide (CPW) multiline thru-reflect-line (TRL) calibrations [1]: asymmetry in a nominally symmetric short, variations in line length and width, error in the capacitance used to determine and correct the calibration reference impedance, and variations in metal thickness and/or resistivity. Each of these five sources of systematic error corrupts the calibration coefficients calculated by the TRL algorithm, which in turn introduces error into the scattering parameters measured by the calibration.

Reference [2] describes the method we use to predict measurement uncertainty due to the presence of our five sources of systematic error. A perfect TRL calibration based on ideal standards will calculate the actual scattering parameters S_{ij} of a device from uncorrected measurement data. However, an imperfect TRL calibration based on standards with systematic errors will result in calibration coefficients which differ from those of the perfect calibration. Those imperfect calibration coefficients will calculate scattering parameters S_{ij}', which will differ from the actual scattering parameters S_{ij}.

The calibration-comparison method determines an upper bound for $|S_{ij}'-S_{ij}|$ from differences in the perfect and imperfect calibration coefficients when $|S_{ii}| \le 1$ and $|S_{12}\,S_{21}| \le 1$. In this work we present predictions for the upper bounds of [2], which we use throughout this work to quantify uncertainty. We test our predictions by deliberately introducing systematic error into real calibration data, performing a calibration comparison, and comparing our predictions to the resulting bounds.

Finally, we determine bounds for the systematic measurement error of an actual CPW calibration.

REFERENCE-IMPEDANCE AND REFERENCE-PLANE SHIFT

Although systematic errors in calibration standards may affect the calibration coefficients in many ways, the dominant effect is often a change in either the reference impedance or reference plane position of the calibration. For example, the dominant effect of asymmetry in a CPW short standard is a shift in the calibration reference-plane position.

The transmission matrix of an impedance transformer and small section of line is [3]

$$\frac{1}{\sqrt{1-\Gamma^2}}\begin{bmatrix} e^{-\gamma(l'-l)} & 0 \\ 0 & e^{\gamma(l'-l)} \end{bmatrix}\begin{bmatrix} 1 & \Gamma \\ \Gamma & 1 \end{bmatrix}, \qquad \textbf{(1)}$$

where $\Gamma = (Z'-Z)/(Z'+Z)$, γ is the propagation constant in a transmission line, and the length of the line is $l'-l$. The impedance Z at the input is shifted by the impedance transformer to an impedance Z' at the output. The transmission matrix describes the difference between a calibration with reference impedance Z and reference plane position l and a calibration with reference impedance Z' and reference plane l' [2].

When two error boxes relating two calibrations are identical, $|S_{ij}' - S_{ij}|$ is bounded by [2]

$$\left|S_{ij}' - S_{ij}\right| \le B \equiv |T_{11} - T_{22}| + 2|T_{21}| + |T_{12}|, \quad \textbf{(2)}$$

where the T_{ij} are the elements of the transmission matrix relating the two calibrations. Substituting the elements of **(1)** into **(2)** results in

$$B = 3\left|\frac{\Gamma}{\sqrt{1-\Gamma}}\right| + \left|e^{-\gamma(l'-l)} - e^{\gamma(l'-l)}\right|, \quad \textbf{(3)}$$

which is valid for two calibrations which differ only in reference impedance and reference plane position. For small reference impedance and reference plane shifts, we have

$$B \approx 3|\Gamma| + 2|\gamma(l'-l)| \approx 3|\Gamma| + 2\frac{\omega|l'-l|}{c}\sqrt{\frac{1+\epsilon_s}{2}}, \quad \textbf{(4)}$$

where ϵ_s is the relative permittivity of the substrate, ω is the angular frequency, and c is the speed of light. Here we approximated the effective relative dielectric constant ϵ as $\epsilon \equiv -(c\gamma/\omega)^2 \approx (\epsilon_s+1)/2$, which is a reasonable approximation when the loss of the CPW is low and the frequency is not very low.

ASYMMETRICAL SHORT

The TRL method uses a reciprocal standard to set the reference plane for the calibration. The calibration algorithm assumes the reciprocal standard is symmetric: that is, it is identical on both ports.

We use a short for the reciprocal standard in our CPW calibrations. If the short has an offset of an amount Δl in one port, then the reference plane of the calibration will be in error by $\Delta l/2$. Equation **(4)** then predicts the bound

$$B_s \approx 2\frac{\omega|\Delta l|}{c}\sqrt{\frac{1+\epsilon_s}{2}} \quad \textbf{(5)}$$

on $|S_{ij}' - S_{ij}|$.

We tested **(5)** experimentally by modifying the data from the measurement of a symmetric short. To do this, we first corrected the measurement of all of our standards using a multiline TRL calibration. We performed a second TRL calibration with a reference plane setting 5 microns longer than in the first, and recorrected the short data. Then we artificially produced measurement data for our asymmetrical short by combining the S_{11} data from the first calibration with the S_{22} data from the second. Finally, we performed a second-tier calibration using the corrected data to generate a bound on $|S_{ij}' - S_{ij}|$. However, we substituted our artificial asymmetrical short data for the data corrected with no reference-plane offset, deliberately introducing error into the second-tier calibration.

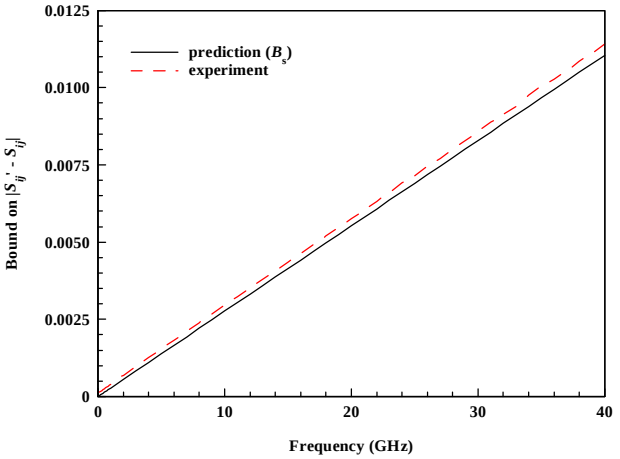

Fig. 1. Predicted error bound B_S for asymmetry in the short standard compared to the experimental value determined with the calibration comparison method of [2].

The dashed line of Fig. 1 compares the original multiline calibration and the second-tier calibration perturbed by using our asymmetrical short data. The bound predicted by **(5)** is plotted as a solid line. There are small differences in the predicted and experimental curves, which may have arisen because we neglected the resistance of the short. Nevertheless, the figure indicates that, at least for low-loss CPW, **(5)** may be used to predict bounds on measurement errors due to asymmetry in the short used in the calibration

LINE-LENGTH ERROR

The multiline method [1] determines the propagation constant γ directly from the measurements of the lines, and uses γ to change the reference-plane position. It also determines the characteristic impedance of the lines from γ using the method of [4], and uses this information to reset the calibration reference impedance to 50 Ω. So errors in γ affect both the final calibration reference impedance and reference-plane position.

The multiline method [1] weights most heavily the measurement of the longest line to determine the propagation constant γ. So if there is an error Δl_l in the length l_l of the longest line, and the reference plane is

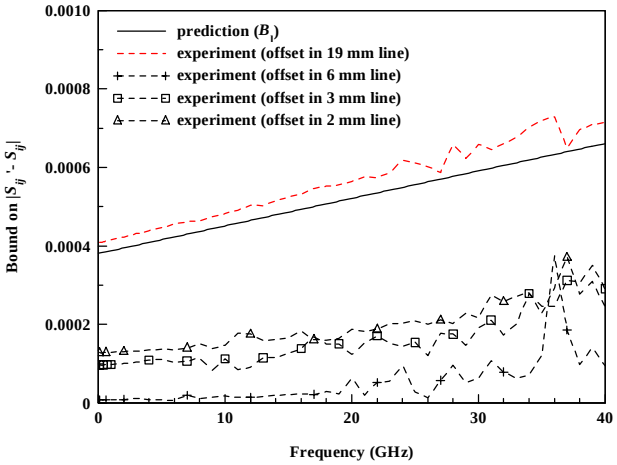

Fig. 2. Predicted error bound B_l for a deviation in the length of the longest line compared to experimental values determined with the calibration comparison method of [2].

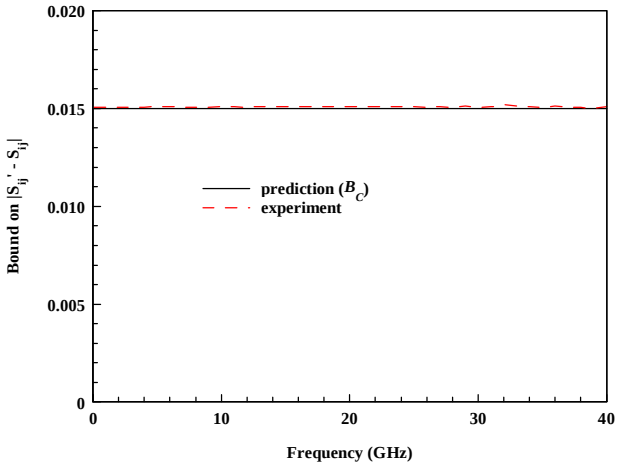

Fig. 3. Predicted error bound B_C for an error in the line capacitance C compared to the experimental value determined with the calibration comparison method of [2].

shifted by Δl_r during the calibration, then **(4)** gives the approximate bound

$$B_l \approx 3\frac{|\Delta l_l|}{2l_l} + 2\frac{\omega|\Delta l_r|}{c}\frac{|\Delta l_l|}{l_l}\sqrt{\frac{1+\epsilon_s}{2}}. \quad \textbf{(6)}$$

We tested **(6)** experimentally by performing a calibration with a long line whose length was incorrect by 5 microns. The dashed line of Fig. 2 shows the error bound of the resulting calibration; the prediction of **(6)** is shown as a solid line. The agreement between prediction and data is good: **(6)** yields approximate bounds on systematic error due to an offset in the length of the longest line.

Also plotted on Fig. 2 are the worst-case errors in the measured data when the length error was in one of the shorter lines used for the calibration. The figure shows that the largest error does indeed occur when the error is in the length of the longest line. This is because the multiline method [1] weights most heavily the measurement of the longest line to determine the propagation constant γ. Thus we see that we can use **(6)** to bound the error due to a change of length of any of the lines in the calibration.

INCORRECT CAPACITANCE

The impedance-correction method of [4] uses the low-frequency capacitance C of the transmission line to calculate its characteristic impedance. If there is an error ΔC in the measurement of C, the characteristic impedance calculated by the algorithm will be incorrect, and **(4)** gives the bound

$$B_C \approx 3\frac{\Delta C}{2C} \quad \textbf{(7)}$$

on the worst-case error in the calibration.

We tested **(7)** experimentally by correcting real measurement data with a calibration performed with a capacitance that was in error by 1%. The worst-case deviation that this error caused is shown as a dashed line in Fig. 3. The solid line in Fig. 3 is the bound on the errors predicted by **(7)**; the prediction agrees well with the experimental result.

VARIATIONS IN LINE WIDTH

An error in the width of a line affects all of the line's parameters. However, the dominant effect is described by a change in the capacitance, and **(7)** can be used to predict the error bound. For the experimental test, we use data from two calibration sets where variations in line width were so large that ΔC was on the order of 10% of C.

The largest error occurred when comparing a normal calibration to a calibration where all of the lines were replaced by devices which differ in width. The dashed line in Fig. 4 shows the bound on the error for this case; the prediction from **(7)** is plotted as a solid line. Agreement is good at low frequency. At higher

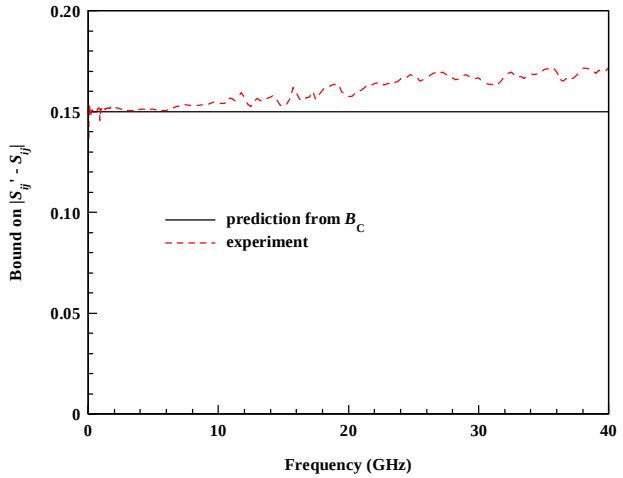

Fig. 4. Predicted error bound B_c for deviations in the line width compared to the experimental value determined with the calibration-comparison method of [2].

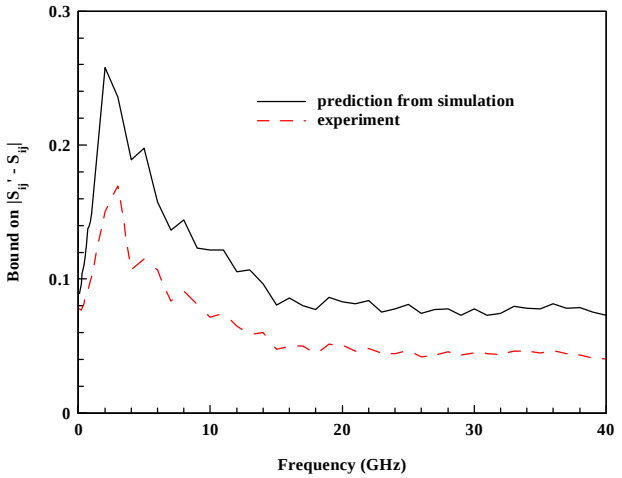

Fig. 5. Predicted error bound from our simulation of deviations in the line resistivity compared to experimental values determined with the calibration-comparison method of [2].

frequencies the measurement data deviate somewhat from the prediction, suggesting the need for a more complete model that includes all of the line parameters. Nevertheless, the figure indicates that for most applications **(7)** will be accurate enough to predict useful bounds on measurement error due to changes in line width.

VARIATIONS IN METAL THICKNESS AND RESISTIVITY

The behavior of errors due to metal thickness and/or resistivity is more complex. Rather than a simple equation, we develop a simulation procedure that predicts the bound on the errors.

First, we make measurements of the dc resistance per unit length R_{dc} of each line. Next, we use real measurements of the calibration devices to estimate the resistance $R(\omega)$ and inductance $L(\omega)$ per unit length of line.

To simulate the calibration, we define a worst-case resistance per unit length $R'(\omega)$, and inductance per unit length $L'(\omega)$ from

$$R'(\omega) = \frac{R_{dc}'}{R_{dc}} R(\omega)$$
$$L'(\omega) = L(\omega) + \frac{R'(\omega) - R(\omega)}{\omega}, \qquad \textbf{(8)}$$

where R_{dc}' is the dc resistance per unit length of line that deviates most greatly from the average dc resistance per unit length of all of the lines. To generate the prediction we perform a simulated calibration in which the longest line has a resistance $R'(\omega)$ and inductance $L'(\omega)$, and all of the other lines have a resistance $R(\omega)$ and inductance $L(\omega)$. Then we generate the bound of [2] by comparing this calibration to one for which all lines have a resistance $R(\omega)$ and inductance $L(\omega)$.

We tested our prediction experimentally by comparing a normal calibration with a calibration made after replacing the measurement of the longest line by the measurement of a line fabricated with metal 4 times thicker. The dashed line of Fig. 5 shows the worst-case deviation of the resulting calibration comparison, with the prediction plotted as a solid line. The good agreement between the prediction and the measurement shows that we can predict the limit on systematic errors due to metal thickness and/or resistivity with the simulation technique.

ESTIMATING WORST-CASE ERROR BOUNDS FOR A TYPICAL CPW CALIBRATION

For our CPW process we estimated that $\Delta l \approx 0.8$ µm (asymmetry in the short), $\Delta l_1 \approx 1.05$ µm (error in line length), $\Delta C/C \leq 1\%$, and $|R_{dc}'-R_{dc}| \approx 3$ Ω/cm. Fig. 6 shows the error bounds predicted by **(5)-(8)** from these values. A sum of the bounds for each error source is

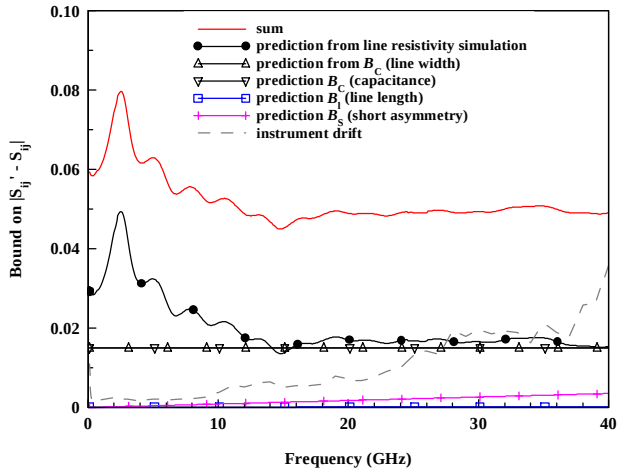

Fig. 6. Predicted bounds for individual sources of error and their sum compared to the bound on errors due to instrument drift for our network analyzer [2].

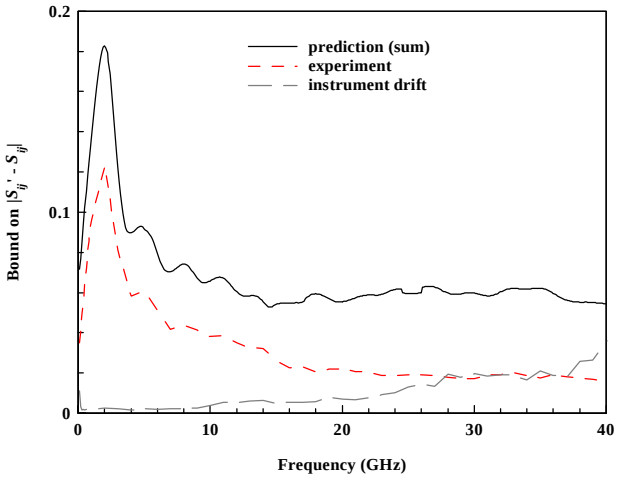

Fig. 7. Predicted error bounds for wafers with uniform and non-uniform metal resistivity compared to the experimental bound determined with the calibration comparison method of [2].

plotted as a solid line and a typical instrument drift is plotted as a dashed line. Fig. 6 shows that in fact our largest error is due to variations in line thickness and/or resistivity.

We tested our ability to predict worst-case error bound by comparing calibrations performed on wafers of uniform and non-uniform resistivity. To determine the contribution of **(8)** to the final sum of errors, the non-uniform line was simulated by cascading 8 separate pieces of line, each with its own R_{dc}' . Fig. 7 compares the sum of all of the predicted errors to the actual bound on the differences between the calibrations found from the calibration comparison method of [2]. The figure shows that the sum of all the errors that we have examined in this paper adequately predicts the upper bound of [2] for our CPW calibrations, and that, when metal resistivity is non-uniform, the error can be significantly larger than the instrument drift at low frequencies.

CONCLUSIONS

We have developed a set of equations which can be used to predict bounds on systematic error in a multiline CPW TRL calibration. For each source of error we demonstrated, through comparisons to actual measurements, that the equations predict the error bound with reasonable accuracy. We also found a total bound on systematic errors by summing the bounds contributed by each error source.

This analysis demonstrated that the largest source of error for our calibrations is due to variations in metal resistivity. This source of systematic measurement error is not usually considered, and may not be apparent unless the calibration is compared to a calibration performed on a wafer with uniform metal resistivity.

ACKNOWLEDGMENTS

The authors would like to thank David Walker for measurement data and Nita Morgan for fabricating test structures, performing analytic measurements, and determining the cause of non-uniform resistivity in the test wafers.

REFERENCES

[1] R.B. Marks, "A Multiline Method of Network Analyzer Calibration," *IEEE Trans. Microwave Theory Tech.*, vol. 39, no. 7, pp. 1205-1215, July 1991.

[2] D.F. Williams, R.B. Marks, and A. Davidson, "Comparison of on-wafer calibrations," *38th ARFTG Conf.*

Dig., pp. 68-81, Dec. 1991.

[3] R.B. Marks and D.F. Williams, "A general waveguide circuit theory," *J. Res. Nat. Inst. of Standards and Technol.*, vol. 97, no. 5, pp. 533-562, Sept. 1992.

[4] R.B. Marks and D.F. Williams, "Characteristic Impedance Determination using Propagation Constant Measurement," *IEEE Microwave Guided Wave Lett.*, vol. 1, no. 6, pp. 141-143, June 1991.